

Serial Post-mortem Relaxometry in the Normal Rat Brain and Following Stroke

Andrew J. Fagan PhD^{1,4}, Jim. M. Mullin HNC^{2,4}, Lindsay Gallagher HNC⁴, Donald M.
Hadley FRCR³, I. Mhairi Macrae PhD⁴, Barrie Condon PhD²

- 1: Department of Medical Physics and Bioengineering, St. James's Hospital, Dublin 8, Ireland.
- 2: Dept. Clinical Physics and Bioengineering, MRI Unit, Institute of Neurological Sciences, Glasgow G51 4TF, UK.
- 3: Dept. Neuroradiology, MRI Unit, Institute of Neurological Sciences, Glasgow G51 4TF, UK.
- 4: 7T MRI Facility, Division of Clinical Neuroscience, Glasgow University Gartnavel Estate, Glasgow G61 1QH, UK.

Corresponding Author:

Dr. Andrew Fagan

Department of medical Physics and Bioengineering,
St. James's Hospital,
Dublin 8,
Ireland.

Tel: +353-1-4162646

Fax: +353-1-4103478

andrew.fagan@tcd.ie

Grant support:

This study was supported by a Research Development Grant from the
Scottish Funding Council.

Running Title:

Post-mortem relaxometry study in rat

Abstract

Purpose: Investigation of MRI for non-invasive autopsy via measurements of serial changes in relaxation parameters of the rat brain during the post-mortem interval.

Materials and Methods: Post-mortem relaxometry measurements were performed before and hourly after death for 24 hours on five control rats and five rats which underwent middle cerebral artery occlusion. Analyses were performed on representative regions of grey, white, and mixed grey/white matter structures.

Results: Significant decreases in both T_1 and T_2 values were measured in all areas in the control group within 24 hours of death. In the stroke animals, T_2 differences between normal and ischaemic striatal tissue decreased by $11 \pm 4\%$ ($p < 0.01$), with a complete convergence of T_2 values observed between ischaemic striatal tissue and non-ischaemic cortical tissue.

Conclusions: Lesion conspicuity and the ability to differentiate between different tissue compartments are significantly affected by post-mortem interval, and alterations to pulse timing parameters will be necessary if the sensitivity of MRI to detect CNS diseases in post-mortem tissue is to be maintained. Indeed in the case of stroke at least, convergence of T_2 values with normal tissue post-mortem indicates that T_1 weighted images may be more sensitive to the presence of such lesions.

Key words: MRI, post-mortem, relaxation times, stroke, autopsy

Introduction

The surgical dissection of the post-mortem corpse (autopsy) has long been recognised as a valuable medical procedure for establishing the cause of death, and the information yielded by autopsies has been invaluable to our understanding of pathology. It has also formed the foundation for medical education and auditing (1,2). Autopsies also allow for the accurate evaluation of treatment methods, can be used to identify new and changing diseases, and have a role to play in forensic investigations and medico-legal issues. However, there has been a marked decline in autopsy rates over the past few decades with, for example, less than 10 % of present-day deaths autopsied in UK teaching hospitals, compared to over 30 % in the 1940's (3). Factors contributing to this decrease include ambivalence toward the procedure by pathologists and clinicians, risks of inoculation from infected patients, issues related to patient / family consent, and restrictions placed by religious doctrines.

The emergence of rapid, high resolution radiological imaging techniques such as x-ray computed tomography (CT) and MRI offer an alternative method of non-invasively assessing the cause of death in situations where an autopsy is not possible. However, while the former is perhaps optimal for assessing bony structures, the soft tissue contrast afforded by MRI would make it a more optimal modality for distinguishing subtle tissue lesions post-mortem. To date, post-mortem studies in humans have predominately involved formalin-fixed tissue, in particular focussing on imaging issues related to maintaining gray / white matter conspicuity following the fixation process (4). However, some examples involving non-fixed tissue have recently been published. These include an investigation of tissue decomposition via ^1H spectroscopy with a view to determining the post-mortem interval (5); forensic investigations in which MRI was used to differentiate and classify the grade of damage following gunshot injury (6); subcutaneous fatty tissue trauma (7); and the use of MRI as an alternative to conventional autopsy (8-10). In this regard, a number of papers have been

published comparing the sensitivity and specificity of MRI and conventional autopsy in the detection of specific abnormalities (for example, see (8-13)). Although close correlations were noted, in general the two approaches have been found to be complementary, with each disclosing abnormalities missed by the other. Study numbers, however, remain small and a recent report commissioned by the UK Department of Health has strongly recommended that more pilot studies be carried out in this area to determine whether MRI can augment or replace conventional autopsy (14).

A number of studies have investigated the use of MRI to image post-mortem formalin-fixed tissue and how relaxation parameters changed with time (4,15-17). In the paper by Tovi and Ericsson (15), the spin-lattice (T_1) and spin-spin (T_2) relaxation values of formalin-fixed brain tissue were found to decrease in the weeks after fixing the tissue, with a convergence of T_1 values in gray and white matter, leading to a loss of contrast in T_1 -weighted MR images. On the other hand, Blamire *et al.* (16) found that the difference in the relative density of protons in gray and white matter increased during the first weeks of fixation, which indicates that optimal gray-white matter contrast may be obtained in formalin-fixed brain tissue using a proton density-weighted protocol. However, it is not clear how relevant these results are to non-fixed tissue, which is more pertinent for the application of MRI for non-invasive autopsy. In particular, formalin fixation is known to change the microstructure of tissue and to have a differential effect on the water mobility of different tissue types (4), giving rise to the observed T_1 and T_2 changes. Changes in water mobility, together with the breakdown of the tissue infrastructure supporting the fibre and vasculature networks, may contribute differently to relaxation changes in non-fixed tissue.

Data on non-fixed tissue are more scarce. In an early study by Gyorffy Wagner *et al.*, the post-mortem changes in excised, non-fixed porcine brain tissue were investigated, with significant changes in T_2 but not T_1 measured up to 90 hours post-mortem (18). However, the excised tissue was maintained at 8 °C throughout the post-mortem interval, while the excision process

was also expected to confound the measured values. The goal of the current study was to measure post-mortem relaxation value changes *in situ*, utilising a more realistic temperature regime, i.e. allowing the animals' temperature to equilibrate to room temperature, which better reflects the typical conditions to which a body will be exposed in the hours after death.

Tissue decomposition occurring during the post-mortem interval, and its consequent effect on tissue relaxation parameters, has a dramatic effect on the image quality in MRI, to the extent that imaging protocols may need to be altered significantly to compensate for the tissue changes, in order to ensure that potential causes of death are not overlooked or falsely reported. Quantification of such tissue changes, which will facilitate modifications of *in vivo* MRI timing parameters to produce optimal *ex vivo* images, must therefore be performed both pre- and post-mortem, necessitating the use of animal models. Although tissue changes occurring in different organs throughout the body will ultimately need to be measured, the present study focused on changes in the brain of both control rats and rats exposed to an experimental stroke prior to death. The results of this study could be used to inform choice of timing parameters in the MRI protocols required to provide a non-invasive autopsy programme in humans.

Materials and Methods

Animals: All experiments were carried out under license from the Home Office and were subject to the Animals (Scientific Procedures) Act, 1986. Ten adult male Sprague-Dawley rats (bodyweights approximately 260 g, Harlan, UK) were anaesthetised, intubated, artificially ventilated and anaesthesia maintained with 1-2 % halothane in 7:3 N₂O/O₂. The rats were divided into two groups of n = 5, consisting of a 'control' group and a second group subjected to an experimental stroke using the Tamura model of electrocoagulation of the proximal middle cerebral artery (MCA) (19). All of the rats were subsequently instrumented for physiological monitoring and transferred to the magnet bore for *in vivo* imaging, before being sacrificed by a halothane overdose of 5 %, four hours after the MCA occlusion. The rats' body temperature was subsequently allowed to equilibrate to the temperature within the gradient bore (25°C).

Imaging: MR imaging experiments were carried out using a 7 T Bruker BioSpec 70/30 system (Bruker, Germany) using an actively shielded gradient set (400 mT/m maximum gradient) with a 72 mm diameter birdcage volume resonator. T₂ weighted imaging was carried out *in vivo* (and at 48 hours after death in one animal) using a RARE sequence (TR/TE = 5000/72 ms, RARE factor 16, 117 µm in-plane resolution, 0.5 mm slice thickness with 30 slices spanning the entire brain). Relaxation measurements were carried out before and beginning 10 minutes after death out to 24 hours (and in one animal out to 48 hrs) post-mortem. Each animal remained in the magnet for the duration of the experiment, with measurements of both T₁ and T₂ carried out every hour. T₁ measurements were performed in an inversion recovery experiment using a segmented FISP readout sequence, in which a series of 20 equi-spaced segmented images were acquired between 60 - 7200 ms after each inversion of the magnetisation, with 8 lines of *k*-space for each image acquired per inversion cycle (in-plane resolution = 312 µm, single coronal slice of thickness 2 mm centred at 1 mm posterior to Bregma according to the Paxinos rat brain atlas (20), acquisition bandwidth =

150 kHz, TR/TE = 3/1.5 ms). The time between successive inversion pulses was set to 8000 ms, to ensure complete recovery of the magnetization to its initial equilibrium value, resulting in an acquisition time of 22 minutes. To reduce errors in the measured T_1 values deriving from the use of an imperfect inversion pulse, adiabatic hyperbolic secant RF inversion pulses were used with a 6 ms duration and a 2.9 kHz bandwidth. A gauss pulse with 5° flip angle, duration 0.8 ms and bandwidth 3.4 kHz was used for the excitation. T_2 measurements were carried out using a multi-slice multiple spin echo technique producing the same spatial resolution over the same slice as in the T_1 measurement sequence in an acquisition time of 15 minutes (TR/TE = 5000/12 ms, acquisition bandwidth = 70 kHz). 20 equi-spaced echo-time images were acquired ranging from 12 to 240 ms, covering the T_2 relaxation period. Both T_1 and T_2 measurement techniques were validated using agar gel phantoms with known relaxation properties (Eurospin Test Objects, Diagnostic Sonar Ltd., UK). Image registration of individual rat brains acquired throughout the post-mortem period was facilitated by adjusting the ^1H frequency of the MRI system every hour, while a standard stereotactic frame (consisting of bite and ear bars) built into the support cradle ensured the heads were fixed securely.

Analysis: T_1 and T_2 parameter fitting was carried out using the Bruker ParaVision software using regions of interest placed over the cortex, corpus callosum, and striatum for measurements of gray, white and mixed white/gray matter regions, respectively (Figure 1). The ParaVision software uses a region of interest based nonlinear least-squares fitting routine to perform a three-parameter fit to the data using the standard equations $I(t) = \alpha + I_0 [1 - 2\exp(-t/T_1)]$ and $I(t) = \alpha + I_0 \exp(-t/T_2)$ for T_1 and T_2 , respectively, where I_0 is the signal intensity from the equilibrium magnetization and α is a bias factor. Error bars in the figures below represent the standard deviation of the mean fitted values from 5 rats. The statistical significance of changes in relaxation values during the post-mortem interval was determined by comparing the mean value just before death with the equivalent value at 24 hours post-mortem using a paired Student's t -test analysis.

Results

T_2 weighted images of the brain of a representative control rat acquired before and 48 hours after death are presented in Figures 2a and 2b, respectively. Some degree of brain swelling within the confines of the skull is evident (of the order of 2 %), together with a loss of signal from the ventricles and also a loss of some gray / white matter differentiation with this duration of post-mortem delay. Histological sections of these brains, post fixed at 48 hours, revealed that ventricles had not collapsed, neuroanatomical landmarks could still be identified and gray and white matter could still be differentiated in haematoxylin and eosin stained sections (data not shown).

Influence of post-mortem delay on T_1 and T_2 values in control brain

The behaviour of the spin-lattice and spin-spin relaxation processes as a function of time post-mortem for corpus callosum (white matter), cortex (gray matter) and striatum (representing gray/white matter mix) in the control group are presented in Figure 3. The data represent mean values from five animals at each time point in this control group. The measured T_1 values, displayed in Figure 3a, exhibit statistically significant decreases from time zero (*in vivo* state just before death) to 24 hours post-mortem ($p < 0.01$). The percentage change over this timeframe was 8, 4 and 6 % (± 2 %) for the corpus callosum, cortex and striatum, respectively. Similarly, the measured T_2 values in these regions decreased significantly over 24 hours post-mortem ($p < 0.001$), with percentage changes of 15, 10, and 16 % (± 2 %), respectively (Figure 3b). Of perhaps more significance, from the point of view of image contrast in MRI, is the differential changes in relaxation values evident between different tissue types which occurred during the post-mortem interval (for example, a comparison of the zero and 24 hour data in Figure 3 shows that the separation of T_1 and T_2 values between gray and white matter increased by 5 ± 3 % and 10 ± 2.5 %, respectively, during this period).

Comparison of temperature loss post-mortem with T_2 change in gray and white matter

The decrease in core body temperature of the rats during the post-mortem interval, as measured using a rectal thermometer, is also plotted in Figure 3 beside the measured T_1 and T_2 values. It can be seen from these graphs that the observed decreases in relaxation values reflect the decreasing temperature during the first 10 hours post-mortem. However, with the exception of the T_1 values measured in the cortex, the relaxation values continued to exhibit a statistically significant decrease ($p < 0.05$ for T_1 , and $p < 0.01$ for T_2 data) after the rats' core temperature had stabilised at approximately 10 hours post-mortem.

Influence of post-mortem delay on T_1 and T_2 values in ischaemic versus non-ischaemic brain

Proximal middle cerebral artery occlusion created a consistent pattern of ischaemic damage in the ipsilateral striatum with more variable damage in the cortex, as indicated in diffusion-weighted images acquired 3 hours post-ischaemia in the living rat (data not shown). Regions of interest in the ipsilateral and contralateral striatum were compared to identify differences in T_1 and T_2 values between ischaemic and non-ischaemic tissue, and how this was influenced by post-mortem delay (Figure 4). Higher T_1 values were recorded in ischaemic striatum compared to non-ischaemic striatum *in vivo* and post-mortem, with maximal differences recorded immediately prior to anaesthetic overdose. It can be seen in Figure 4a that the T_1 values of the ischaemic striatum exhibited a similar decrease over time as compared to the non-ischaemic tissue (decreases of the order of $8 \pm 3\%$ and $5 \pm 1.5\%$, respectively from time 0 to 24 hours post-mortem, both statistically significant at $p < 0.01$), with a small differential change ($< \sim 3\%$) measured over this time period. The maximum difference in T_2 values between ischaemic and non-ischaemic striatum was evident 1 hour after death due to the initial rapid drop in T_2 in non-ischaemic tissue (also evident in the control group, Figure 3b) which was not reflected to the same extent in ischaemic striatum (Figure 4b). T_2 values decreased significantly ($p < 0.001$) in ischaemic and non-ischaemic tissue by 18% and 15%

($\pm 3.5\%$), respectively, over the 24 hour post-mortem period, with a differential change between these tissues of the order of $11 \pm 4\%$ over this period.

To illustrate how a significant post-mortem change in relaxation values will have a clear effect on image contrast, we present in Figure 5 data to illustrate the relaxation changes that might be expected in ischaemic striatal tissue adjacent to non-ischaemic cortical tissue. To ensure that the data used were characteristic of normal cortex, rather than ischaemic cortex, the region of interest used for measurements of the cortical tissue was placed on the contralateral hemisphere (region 2 in Figure 1, with the ischaemic striatal damage typically occurring in region 4); nevertheless, similar values would be expected from non-ischaemic cortical tissue neighbouring the ischaemic striatal tissue. It is clear from Figure 5(a) that the measured T_1 values for both regions are similar *in vivo*, but become divergent during the post-mortem interval. T_2 values, on the other hand, are clearly different *in vivo* but converge with time post-mortem (Figure 5(b)); indeed, at 24 hours post-mortem, T_2 contrast is completely lost between these tissue types.

Discussion

This is the first study to report significant serial changes in the relaxation parameters of *in situ* brain tissue following death. Rather than finding an increase in T_1 and T_2 values post-mortem, as might be expected if the tissue loses its structure and becomes more oedematous, decreases in both parameters were actually revealed with post-mortem delay. The reason for this is not clear but it may indicate a change of compartment of water molecules between extra- and intra-cellular compartments. A changing magnetic state of blood from dia- to paramagnetic, as O_2 is released from haemoglobin molecules in the decomposing blood, may also contribute to the observed effects. Previous studies have observed a similar decrease in T_1 values associated with the coagulation of blood in excised tissue samples and human blood specimens (21); the authors related this altered T_1 relaxation to increased access of water molecules to paramagnetic relaxation centers in the blood following haemoglobin denaturing and cell membrane rupturing. It is interesting to note that the striatal T_2 values in the control group (Figure 3b) exhibit a more pronounced decrease during the post-mortem interval compared to the cortex and corpus callosum. Further experiments will be required to elucidate the origins of this finding.

The average body temperature of the rats dropped rapidly in the immediate hours after death, equilibrating to the temperature within the gradient bore after approximately 10 hours. This loss of body temperature after death is an additional confounding factor which can be expected to influence T_1 relaxation values and, consequently, any clinical application of MRI post-mortem. Indeed, temperature-induced changes in T_1 relaxation values were predicted by the classic Bloembergen-Purcell-Pound (BPP) theory (22), and have been exploited in a number of studies to map temperature changes *in vivo* (23,24) and in autopsied samples (25). For a simple homogenous system, the BPP theory describes the T_1 relaxivity as follows:

$$\frac{1}{T_1} \propto \left[\frac{2\tau_c}{1 + \omega_0^2 \tau_c^2} + \frac{8\tau_c}{1 + 4\omega_0^2 \tau_c^2} \right]$$

where ω_0 is the NMR frequency and τ_c is the correlation time associated with the fluctuating local field, which is inversely related to the temperature. The situation is complicated in tissue, which is a highly heterogeneous environment, leading to a more complicated dependence of T_1 on both magnetic field strength and temperature. Empirical studies carried out at relatively low field strengths used clinically (≤ 1.5 T) indicate an approximate linear temperature dependence across the physiological to room temperature range, varying from 1% change per °C (26) to 1.3-1.5 % change per °C (25), with a strong dependence on the specific tissue type under investigation. However, the lack of similar data in the rat brain at the higher field strength used in the current study renders it difficult to predict an expected decrease in T_1 values associated with the temperature decrease observed during the post-mortem period. Nevertheless, it is interesting to note that the T_1 values for the corpus callosum and striatum continued to decrease after the animals' core temperature had stabilised (Figure 3), indicating that temperature alone does not account for the observed decreases. This is the first time that a non-temperature related decrease in T_1 values has been reported; in a previous study on excised porcine brain tissue, no decrease was observed, although a complicated temperature regime was utilised (involving the storage of tissue at 8°C throughout the post-mortem interval and its reinstatement to room temperature for the relaxometry measurements) which, coupled with the excision process, may have influenced the measurements (18). By avoiding any interference with the brain during the post-mortem interval, and using a realistic temperature regime (i.e. allowing the body to cool to room temperature naturally), the current study aimed to remove such potential confounds. Further, the current study allowed us to compare relaxation changes in different brain structures, compared to the bulk relaxometry measurements carried out previously.

In the clinical situation temperature effects will be far more variable as corpses are often refrigerated soon after death. Corpses presented for imaging fresh from the mortuary will be rising in temperature, while those taken to the MR immediately from the ward will be

decreasing in temperature. Our results indicate that at some post-mortem intervals T_2 contrast may be reduced significantly between, for example, non-ischaemic and ischaemic striatum, or indeed ischaemic striatum and adjacent non-ischaemic cortex, if *in vivo* pulse timing parameters are maintained. It may therefore be necessary to take body temperature into account and use this to alter timing parameters to enhance diminishing contrast.

Ultimately, however, if the convergence of T_2 values becomes too close it may be necessary to resort to T_1 weighted imaging. *In vivo* T_2 weighted imaging is used as a sensitive indicator of the presence of disease as it produces good contrast between lesions and normal tissue.

However, even within 8 hours post-mortem, the significant convergence of T_2 values congruent with the maintenance or increasing differential of T_1 values (Figure 5), may mean that T_1 weighted imaging becomes more sensitive for this task.

In conclusion, the results presented in this preliminary study indicate that imaging sequences conventionally optimised for *in vivo* imaging cannot be seamlessly translated to imaging in the *ex vivo* state, and pathologies which may be readily apparent *in vivo* may exhibit significantly diminished contrast post-mortem, with the associated risk that they might be overlooked during a virtual autopsy performed via MRI, particularly where the sequences are weighted towards T_2 . Although the current study focussed on the rat brain at 7 T and one particular pathology (i.e. stroke), it can nonetheless be expected that significant effects will likewise be encountered at the lower field strengths used clinically. Indeed, the prediction of the BPP theory of an increased dependency of T_1 on temperature at lower field strengths would in itself suggest a larger decrease in T_1 values compared to that observed in the current study. Further studies are required to determine the applications and limitations of post-mortem MRI, to extend these studies in gyrencephalic species and at lower field strength (e.g. 1.5 T), and to delineate post-mortem changes in normal versus diseased tissue throughout the body and across a range of pathologies. The use of animal models greatly simplify this task, not least in obtaining adequate sample numbers for such studies, but also since this approach

allows for the comparison of changes in normal and diseased tissue differentiation pre- and post-mortem and for the investigation of the influence of parameters such as body temperature.

Acknowledgments

The authors would like to thank Professor David Graham for neuropathological assessment of post-fixed brain tissue.

References

1. Hill RB, Anderson RE. The recent history of the autopsy. *Arch Pathol Lab Med* 1996;120:702-712.
2. AMA Council on Scientific Affairs. Autopsy: a comprehensive review of current issues. *Arch Pathol Lab Med* 1996;129:721-726.
3. Perkins GD, McAuley DF, Davies S, Gao F. Discrepancies between clinical and postmortem diagnoses in critically ill patients: an observational study. *Crit Care Med* 2003;7:R129-R132.
4. Pfefferbaum A, Sullivan EV, Adalsteinsson E, Garrick T, Harper C. Postmortem MR imaging of formalin-fixed human brain. *Neuroimage* 2004;21:1585-1595.
5. Ith M, Bigler P, Scheurer E et al. Observation and identification of metabolites emerging during postmortem decomposition of brain tissue by means of in situ H-1-magnetic resonance spectroscopy. *Magn Reson Med* 2002;48:915-920.
6. Thali MJ, Yen K, Schweitzer W et al. Virtopsy, a new imaging horizon in forensic pathology: Virtual autopsy by postmortem multislice computed tomography (MSCT) and magnetic resonance imaging (MRI) - a feasibility study. *J Forensic Sci* 2003;48:386-403.
7. Yen K, Vock P, Tiefenthaler B et al. Virtopsy: Forensic traumatology of the subcutaneous fatty tissue; Multislice computed tomography (MSCT) and magnetic resonance imaging (MRI) as diagnostic tools. *J Forensic Sci* 2004;49:799-806.
8. Bisset RAL, Thomas NB, Turnbull IW, Lee S. Postmortem examinations using magnetic resonance imaging: four year review of a working service. *BMJ* 2002;324:1423-1424.

9. Patriquin L, Kassarian A, Barish M et al. Postmortem whole-body magnetic resonance imaging as an adjunct to autopsy: Preliminary clinical experience. *J Magn Reson Imaging* 2001;13:277-287.
10. Ezawa H, Yoneyama R, Kandatsu S, Yoshikawa K, Tsujii H, Harigaya K. Introduction of autopsy imaging redefines the concept of autopsy: 37 cases of clinical experience. *Pathol Int* 2003;53:865-873.
11. Hart BL, Dudley MH, Zumwalt RE. Postmortem cranial MRI and autopsy correlation in suspected child abuse. *Am J Forensic Med Pathol* 1996;17:217-224.
12. Whitby EH, Variend S, Rutter S et al. Corroboration of in utero MRI using post-mortem MRI and autopsy in fetuses with CNS abnormalities. *Clin Radiol* 2004;59:1114-1120.
13. Roberts ISD, Benbow EW, Bisset R et al. Accuracy of magnetic resonance imaging in determining cause of sudden death in adults: comparison with conventional autopsy. *Histopathology* 2003;42:424-430.
14. Parker A. Less Invasive Autopsy, the Place of Magnetic Resonance Imaging, report commissioned by the Policy Research Programme of the Department of Health. 2004:
15. Tovi M, Ericsson A. Measurements of T1 and T2 Over Time in Formalin-Fixed Human Whole-Brain Specimens. *Acta Radiol* 1992;33:400-404.
16. Blamire AM, Rowe JG, Styles P, McDonald B. Optimising imaging parameters for post mortem MR imaging of the human brain. *Acta Radiol* 1999;40:593-597.
17. Schumann CM, Buonocore MH, Amaral DG. Magnetic resonance imaging of the post-mortem autistic brain. *J Autism Dev Disord* 2001;31:561-568.
18. Gyorffy-wagner Z, Englund E, Larsson EM, Brun A, Cronqvist S, Persson B. Proton Magnetic-Resonance Relaxation-Times T1 and T2 Related to Postmortem Interval - An Investigation on Porcine Brain-Tissue. *Acta Radiol-Diag* 1986;27:115-118.

19. Tamura A, Graham DI, McCulloch J, Teasdale GM. Focal Cerebral-Ischemia in the Rat
.1. Description of Technique and Early Neuropathological Consequences Following
Middle Cerebral-Artery Occlusion. *J Cereb Blood Flow Metab* 1981;1:53-60.
20. Paxinos G, Watson C. The rat brain in stereotaxic coordinates, 4th edition. New York:
Academic Press; 1998.
21. Graham SJ, Stanisz GJ, Kecojevic A, Bronskill MJ, Henkelman RM. Analysis of changes
in MR properties of tissues after heat treatment. *Magn Reson Med* 1999;42:1061-1071.
22. Bloembergen N, Purcell EM, Pound RV. Relaxation effects in nuclear magnetic
resonance absorption. *Phys Rev* 1948;73:679-721.
23. Parker DL, Smith S, Sheldon P, Crooks LE, Fussel L. Temperature distribution
measurement in two dimensional NMR imaging. *Med Phys* 1983;10:321-325.
24. Moser E, Winklmayr E, Holzmüller P, Krssak M. Temperature and pH-dependence of
proton relaxation rates in rat liver tissue. *Magn Reson Imaging* 1995;13:429-440.
25. Koenig SH, Brown RD, Spiller M, Lundbom N. Relaxometry of brain - why white matter
appears bright in MRI. *Magn Reson Med* 1990;14:482-495.
26. Lewa CJ, Majewska Z. Temperature relationships of proton spin-lattice relaxation time-
T1 in biological tissues. *Bull Cancer* 1980;67:525-530.

Figure legends



Figure 1: An *in vivo* T₂-weighted image to illustrate the positioning of regions of interest over the cortex (1, 2), corpus callosum (3) and striatum (4, 5).

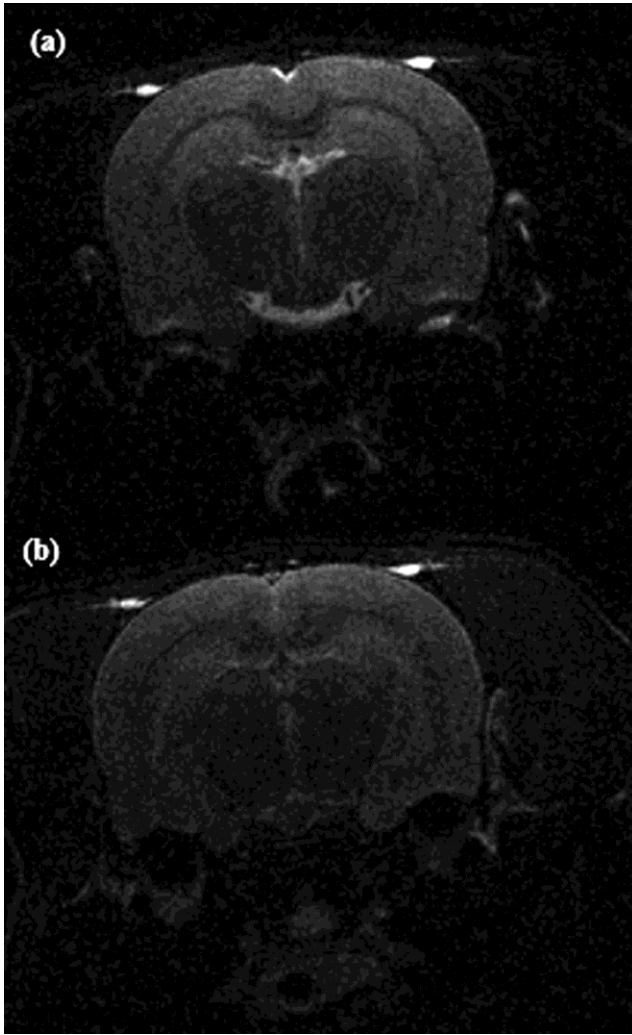


Figure 2: T₂ weighted images of the same brain slice acquired (a) before and (b) 48 hours after death in a control rat.

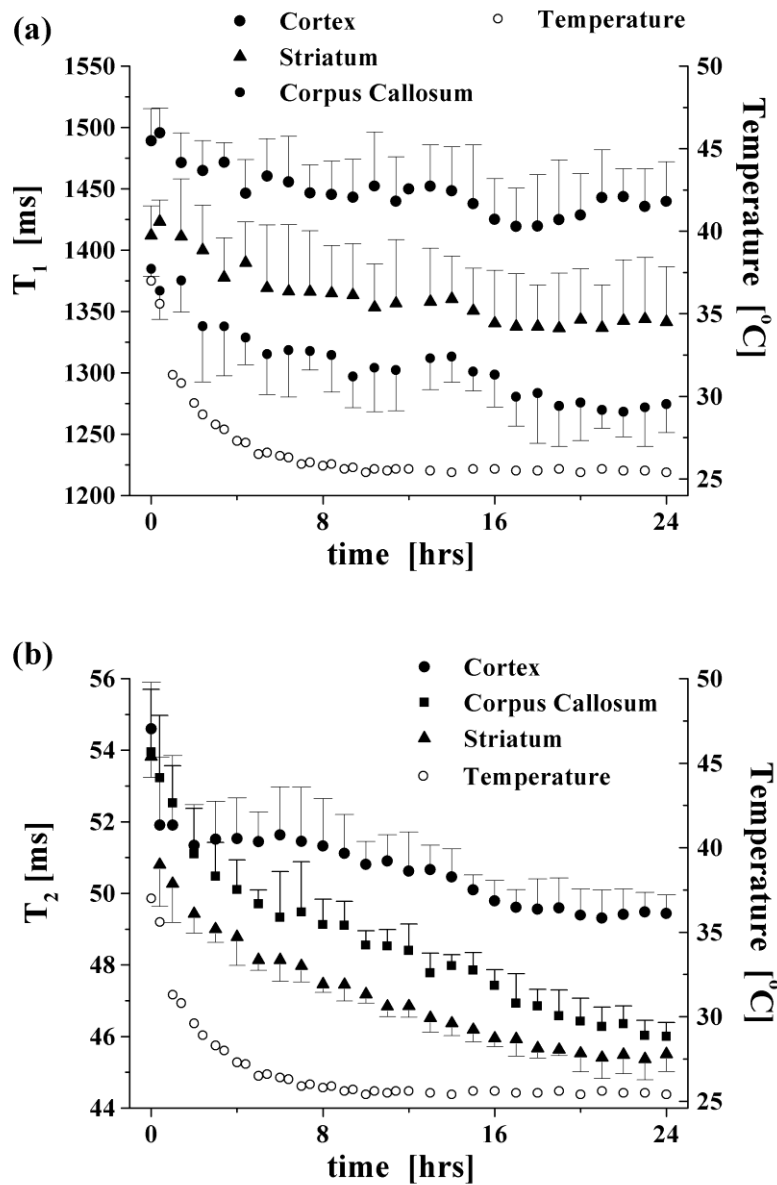


Figure 3: (a) T_1 and (b) T_2 relaxation time measurements as a function of time post-mortem in the control group, contrasting changes in gray and white matter as measured using regions of interest placed over the cortex, striatum (mixed gray and white matter) and corpus callosum. The first data point (at time = 0) represents the *in vivo* state. The data represents a mean of $n = 5$ animals, with error bars representing either + or - standard deviation, for clarity. The drop in core body temperature of the rats during the post-mortem interval is also illustrated.

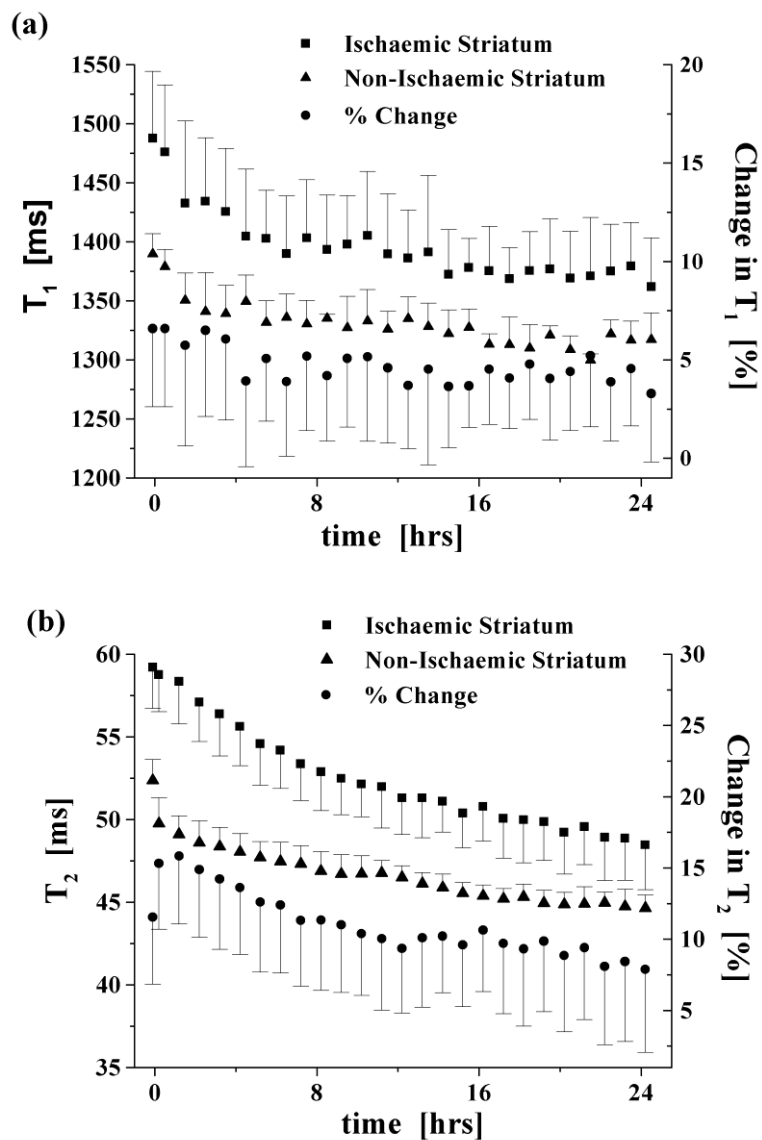


Figure 4: Changes in (a) T_1 and (b) T_2 between ischaemic striatum and contralateral, non-ischaemic striatum as a function of time post-mortem in absolute and differential terms ($n = 5$, with error bars representing either + or - standard deviation, for clarity). The first data point displays *in vivo* T_1 and T_2 values 4 hours after stroke.

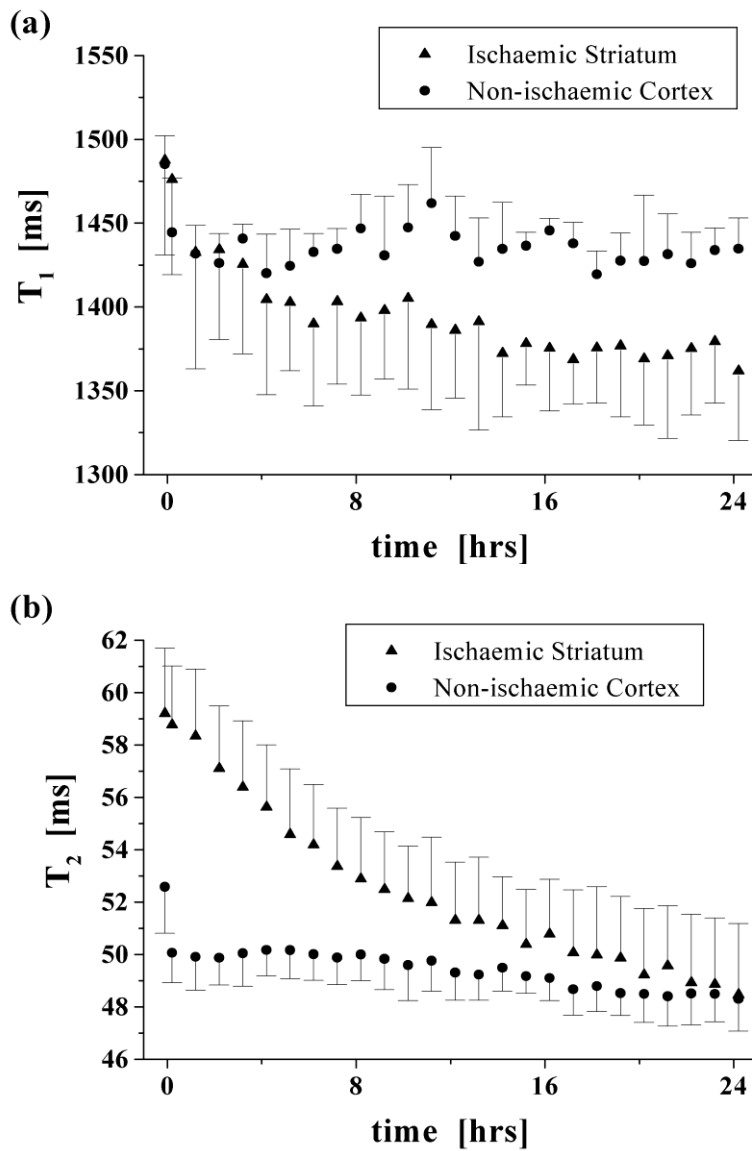


Figure 5: (a) T_1 and (b) T_2 changes as a function of time post-mortem, illustrating the gain/loss of contrast, respectively, between two tissue compartments: non-ischaemic cortical tissue and ischaemic striatal tissue ($n = 5$, with error bars representing either + or – standard deviation, for clarity).